Calculation of electronic, structural, and vibrational properties in alkali halides using a density-functional method with localized densities

W. N. Mei
Department of Physics, University of Nebraska at Omaha, Omaha, Nebraska 68182-0266

L. L. Boyer and M. J. Mehl
Center for Computational Materials Science, Naval Research Laboratory, Washington, D.C. 20375-5345

M. M. Ossowski
Department of Physics, University of Nebraska at Lincoln, Lincoln, Nebraska 68588

H. T. Stokes
Department of Physics and Astronomy, Brigham Young University, Provo, Utah 84602
(Received 7 December 1999)

A recently developed density-functional method based on localized densities is applied to calculate electronic, structural, and vibrational properties of 20 alkali halides with elements lithium through cesium and fluorine through iodine. Properties calculated include dissociation energy, lattice parameter, dielectric constant, elastic moduli, and phonon frequencies for the high-symmetry points of the Brillouin zone. Results are discussed and compared with experiment and other calculations.

I. INTRODUCTION

An approach to first-principles studies for ionic solids based on localized densities has been presented in a recent series of papers.[1–5] In this method the densities are obtained by solving one-electron Schrödinger's equations, one for each atomic site, whose potentials are determined variationally from the total energy. A local-density approximation[6] is employed to account for exchange and correlation energy and kinetic energy contributions due to overlapping densities are included using the Thomas-Fermi approximation. The Schrödinger's equations are solved using basis functions with radial dependence given by tabulated Slater functions[7,8] and angular dependence given by spherical harmonics. Since the potentials are nonspherical in general, so also are the resultant atomic/ionic densities. The new densities determine a new set of potentials and the procedure is iterated to self-consistency. For this reason the method is called self-consistent atomic deformation (SCAD). As a result of the variational formulation of the potentials the SCAD method automatically minimizes the total energy in accord with Janak's theorem.[9]

The SCAD method can be viewed as an extension of the Gordon-Kim[10] model which allows for complete relaxation of the atomic densities. Several other self-consistent atomic models have been presented.[11–17] The SCAD method evolved from attempts to extend the work of Edwardson.[14] It is closely related to the approach taken by Ivanov and Maksimov[17] and appears to be formally equivalent to that of Cortona.[16] However, Cortona's applications[18] were limited to consideration of spherically symmetric charge relaxations. Lacks and Gordon[19] have used a direct energy minimization technique to obtain impressive results for several oxides. Their approach accounts for nonspherical ions by incorporating spherical bonding charges between spherical ions.

Applications of the SCAD method for oxide-based perovskite materials have been encouraging and have thrown new light on the origins of ferroelectric instabilities in these systems.[4,5] Most recently, it was applied to calculate polarization and related properties for one compound selected from each of the I-VII, II-VI, and III-V groups.[21] Results obtained for the selected I-VII compound (NaCl) were in especially good agreement with experiment.

In this work we continue these studies by doing a thorough investigation of the I-VII (alkali-halide) compounds, which are expected to be most accurately described by SCAD. In particular, we report results for dissociation energy, lattice parameter, elastic moduli, dielectric constant, Born effective charges, optic mode frequencies, and frequencies at other high-symmetry points of the Brillouin zone for the 20 compounds lithium through cesium and fluorine through iodine.

II. METHOD

The SCAD method has been described in previous publications.[2–4] We proceed here with a brief account. The total energy is written

$$E[n(\mathbf{r})]=\sum_i T_0[n_i(\mathbf{r})]+T_k[n(\mathbf{r})] - \sum_i T_k[n_i(\mathbf{r})]+F[n(\mathbf{r})], \quad (1)$$

where the total density is given by a sum over site localized densities, each expressed as spherical harmonic expansions about the atomic sites $\mathbf{R}_i$:

$$n(\mathbf{r})=\sum_i n_i(\mathbf{r}-\mathbf{R}_i)=\sum_{i,l,m} n_{lm}^{(i)}(|\mathbf{r}-\mathbf{R}_i|)Y_{lm}(\widehat{\mathbf{r}-\mathbf{R}_i}). \tag{2}$$

The densities associated with each site (n_i) and the on-site kinetic energies ($T_0[n_i]$) are determined from the occupied solutions of Schrödinger's equation for the potential formulated variationally from the total energy[2]

$$v_i(\mathbf{r})=v_F[n(\mathbf{r})]+v_k[n(\mathbf{r})]-v_k[n_i(\mathbf{r})]=\sum_{l,m} v_{lm}^{(i)}(r)Y_{lm}(\hat{\mathbf{r}}), \tag{3}$$

where $\mathbf{r}$ is with respect to an origin at site i. In the above expressions, T_k is a functional to account for the kinetic energy due to overlapping densities (the Thomas-Fermi expression is used here), F denotes all nonkinetic (i.e., exchange-correlation[6] and electrostatic) contributions to the total energy and $v_F(v_k)$ are the functional derivatives of $F(T_k)$.

The Schrödinger's equations are solved using a basis composed of tabulated radial Slater-type functions[7,8] times the corresponding spherical harmonics. Additional Y_{lm}'s (up to $l=3$) are included for radial functions of the valence electrons (negative ion p states). This results in terms up to $l=6$ in the spherical harmonic expansion of the densities. We find the density expansion can be truncated at $l=4$, along with the potential expansion, with negligible error. Once convergence is achieved (typically in ~ 20 iterations mixing 40% of the new and 60% of the old charge densities) Eq. (1) is evaluated for the total energy. Long-ranged contributions to the energy and potentials are determined using Ewald techniques for interactions among monopoles, dipoles, and quadrupoles. The particular methods employed for computing the various properties reported here are discussed as part of Sec. IV below.

III. POLARIZATION

The method for computing polarization within the SCAD model is straightforward.[21] We can adopt the usual definition of polarization, as the dipole moment per unit volume. In general, this quantity is only defined to within a constant; because, for a finite crystal, its value will depend on surface structure. However, the *change* in polarization of a crystal is given unambiguously by its *change* in dipole moment,

$$\Delta\mathbf{P}=\Delta\mathbf{p}_c/V_c, \tag{4}$$

where $\mathbf{p}_c(V_c)$ is the dipole moment (volume) *of the crystal*. In the SCAD model the total charge density is expressed as a sum over ''atomiclike'' densities [Eq. (2)] with monopoles and dipoles determined self-consistently. For the compounds considered here, the monopole charge of each ion remains $+1$ or -1, and the dipole moment of each ion is determined by SCAD. Our unit cell is defined, as in crystallography, by identifying the space group and Wyckoff positions of the ions. Thus the change in dipole moment of the unit cell is given straightforwardly in terms of the displacement of the monopole charges and the change in the dipole moments of the ions. Moments of charge are determined by integrations *over all space*. By assumption, our crystal has no net charge, so its dipole moment is independent of the origin. Moreover, its value is given uniquely (to within a constant depending on the particular arrangement of monopoles on the surface) by the sum of the dipole moments of the ions. If the number N of unit cells in the crystal is large, then we can write

$$\Delta\mathbf{p}_c=N\Delta\mathbf{p}, \tag{5}$$

where $\Delta\mathbf{p}$ is the change in the dipole moment of a unit cell in the bulk, and

$$\Delta\mathbf{p}_c/V_c=\frac{1}{V}\sum_i \Delta\mathbf{p}_i, \tag{6}$$

where $\mathbf{p}_i$ is the dipole moment of the ith ion and $V=V_c/N$ is the volume per unit cell.

If we had attempted to define the dipole moment of a unit cell by integrating over some region of space with volume V, then the definition of $\Delta\mathbf{p}$ would be ambiguous, as pointed out by Martin.[22] The ambiguity results from a lack of accounting for charge that may flow from one unit-cell volume (V) to another. The ''modern theory of polarization''[23] successfully deals with this problem by defining change in polarization in terms charge flow. This allows computation of $\Delta\mathbf{P}$ from quantities derived from the Kohn-Sham[24] (KS) band-structure approach, in which the charge density is expressed in terms of functions that are extended throughout the crystal. An ambiguity in our expression for $\Delta\mathbf{P}$ would arise if charge were to be transferred from one ion to another; a situation analogous to that discussed by Martin. However, this could only happen if the SCAD energy levels of the valence electrons were not completely occupied. In our case the halide p states *are* completely occupied, and the next higher unoccupied levels are well above these in energy (Table I).

TABLE I. Calculated and experimental (Ref. 20) values for band gaps in eV. Experimental values are shown in parentheses.

	Li	Na	K	Rb	Cs
F	11.5(12.6)	10.3(11.7)	5.0(10.9)	6.8	5.5
Cl	7.5(9.4)	6.7(7.3)	5.1(7.2)	5.7(7.3)	5.1(7.6)
Br	7.2	6.6(7.1)	5.3(6.6)	5.7(6.3)	5.2(6.6)
I	5.6	5.1(5.4)	4.2(5.5)	4.6(5.8)	4.2(5.6)

IV. RESULTS AND DISCUSSION

The unoccupied s levels of the alkali ions are found to be several eV above the highest occupied levels (p states) of the halide ions. Thus, the monopole charges are predicted by SCAD to be $+1$ for the alkali ions and -1 for the halide ions. Transferring charge from the halide ion's outer p level to the alkali ion's lowest unoccupied level produces a sharp increase in energy. As is often done in presentations of band-structure results based on the KS formulation of density-functional theory, we compare the energy difference between the highest occupied and lowest unoccupied levels with experimentally determined band gaps. There is no fundamental reason to expect a good correlation in either case because the Hohenberg-Kohn theorem[25] makes no statement about the possible significance of one electron energy levels used in

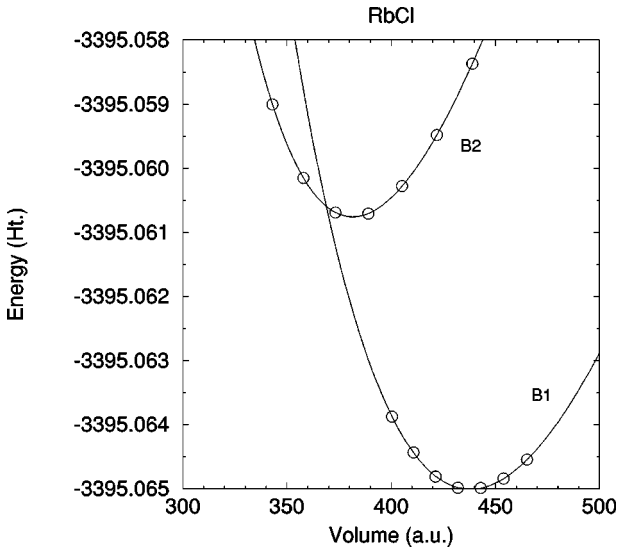

FIG. 1. SCAD total-energy values (circles) and four-parameter Birch fit (solid lines) for RbCl in the B1 and B 12structures.

the determination of the density. In fact, band gaps from KS calculations tend to underestimate experimental values by about 30% to 50%. As seen in Table I, we find a somewhat better correlation with experimental values, although the calculated values are substantially too low for the potassium compounds. We would expect a larger band-gap prediction from the SCAD method compared to results of band-structure calculations, simply because the width of bands centered about the SCAD energy levels would reduce the band-gap values.

Elastic moduli and phonon frequencies are derived from the dependence of total energy as a function of small distortions of the crystal structure. For all but the lithium compounds we were able to choose distortions with displacements of ~ 0.01 to ~ 0.1 Bohr for the total-energy calculations. For the lithium compounds, however, the total-energy results displayed some noise that could produce large errors when using small ($< \sim 0.1$ Bohr) displacements. Further examination showed the noise to be somewhat sensitive to small changes in the radial basis functions.[26] We do not have an explanation for this except to suggest that it may be related to the fact that the Li^+ ion does not have a core. For the other alkali ions, the density which overlaps most strongly with the negative ions is partially stabilized by orthogonalization with its core electrons. In any case, we have attempted to avoid this problem by including more and larger distortions for the lithium compounds to compute phonon frequencies. This is discussed in more detail below. While this strategy was reasonably successful, we still find significantly larger errors for the lithium compounds.

The equilibrium lattice parameters (a) and bulk moduli (B) were determined, as described by Mehl *et al.*,[27] from a four parameter Birch equation fitted to 6–8 total-energy values in the region of the energy minimum. The quality of the fit is illustrated in Fig. 1 where the total energy for RbCl is plotted as a function of volume for both B1 (rock salt) and B2 (CsCl) structures. The smooth behavior of the total-energy values as a function of volume, illustrated in Fig. 1, is typical for all compounds treated, including the lithium halides. Calculated values for lattice parameter a and bulk modulus B, derived from the Birch fit, are listed in Table II

TABLE II. Calculated and experimental (Ref. 28) values of lattice constant a in $\dot{A}$, the high-frequency dieletric constant ϵ_∞, Born effective charge Z^*, elastic moduli (bulk modulus B and shear modulii $C_{11}-C_{12}$ and C_{44}) in units of 10^{11} dyn/cm^2 and dissociation energy D in eV. Experimental values are expressed in parentheses.

	a	ϵ_∞	Z^*	B	$C_{11}-C_{12}$	C_{44}	D
LiF	3.99(4.00)	2.03(1.93)	1.14(1.05)	9.24(6.98)	3.74(6.92)	6.30(6.49)	10.2(8.8)
LiCl	4.98(5.08)	2.95(2.79)	1.32(1.24)	4.09(3.34)	1.62(2.94)	2.33(2.67)	7.9(7.1)
LiBr	5.34(5.43)	3.67(3.22)	1.47(1.26)	3.15(2.63)	1.32(2.03)	1.51(2.05)	7.3(6.5)
LiI	5.74(6.00)	4.68(3.80)	1.64(1.36)	2.60(1.92)	1.16(1.45)	1.02(1.41)	6.7(5.6)
NaF	4.64(4.63)	1.63(1.70)	1.07(1.02)	5.62(5.14)	8.27(8.56)	3.10(2.90)	8.9(7.8)
NaCl	5.58(5.64)	2.26(2.25)	1.15(1.12)	2.54(2.66)	4.00(4.61)	1.12(1.33)	6.9(6.6)
NaBr	5.96(5.98)	2.67(2.60)	1.17(1.13)	2.07(2.26)	3.34(3.81)	1.05(1.07)	6.4(6.0)
NaI	6.40(6.47)	3.15(3.15)	1.23(1.2)	1.74(1.79)	2.97(2.96)	0.67(0.78)	5.8(5.2)
KF	5.21(5.35)	1.78(1.50)	1.21(1.21)	4.07(3.51)	6.36(6.11)	1.73(1.29)	8.6(7.6)
KCl	6.08(6.29)	2.35(2.10)	1.23(1.16)	2.06(1.97)	3.62(4.29)	0.81(0.66)	7.2(6.7)
KBr	6.37(6.6)	2.65(2.43)	1.27(1.19)	1.83(1.77)	3.14(3.62)	0.63(0.53)	6.7(6.2)
KI	6.77(7.07)	3.04(2.70)	1.32(1.15)	1.54(1.27)	2.74(3.16)	0.42(0.37)	6.2(5.4)
RbF	5.52(5.63)	1.88(1.90)	1.27(1.26)	3.45(2.93)	5.34(5.42)	1.33(0.94)	8.6(7.4)
RbCl	6.39(6.58)	2.36(2.23)	1.24(1.10)	1.73(1.95)	3.29(3.82)	0.65(0.50)	7.3(6.6)
RbBr	6.65(6.89)	2.59(2.41)	1.27(1.15)	1.66(1.60)	3.05(3.39)	0.56(0.41)	6.9(6.1)
RbI	7.04(7.34)	2.91(2.63)	1.31(1.29)	1.38(1.31)	2.63(2.85)	0.34(0.29)	6.4(5.4)
CsF	5.89(6.01)	2.06(2.18)	1.38(1.28)	2.91(2.67)	4.57(5.09)	1.07(0.79)	8.6(7.3)
CsCl	3.99(4.11)	2.96(2.60)	1.44(1.26)	2.11(1.98)	3.68(2.37)	0.37(1.08)	7.7(6.6)
CsBr	4.13(4.29)	3.16(2.70)	1.5(1.19)	1.83(1.8)	3.22(2.33)	0.41(1.00)	7.2
CsI	4.33(4.56)	3.63(3.00)	1.56(1.11)	1.71(1.44)	2.32(1.94)	0.50(0.82)	6.8(5.5)

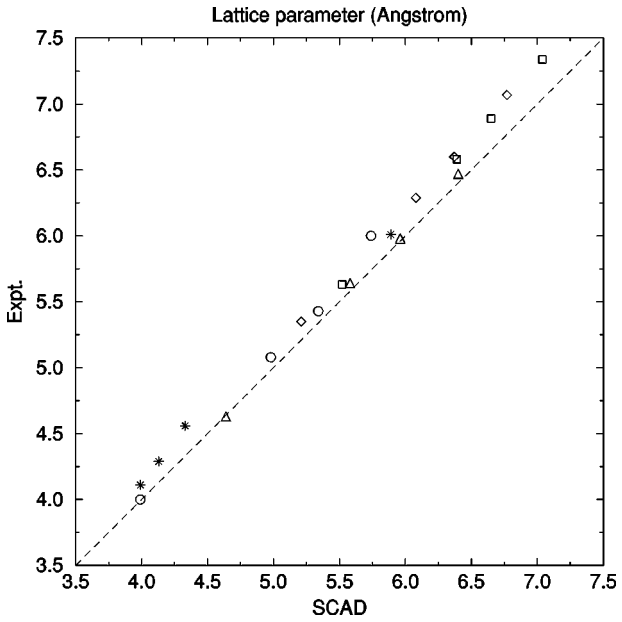

FIG. 2. Calculated vs experimental (Ref. 28) lattice parameters, in angstroms, for the alkali halides: ○-Li;△-Na; ◇ -K;□-Rb; and ∗-Cs.

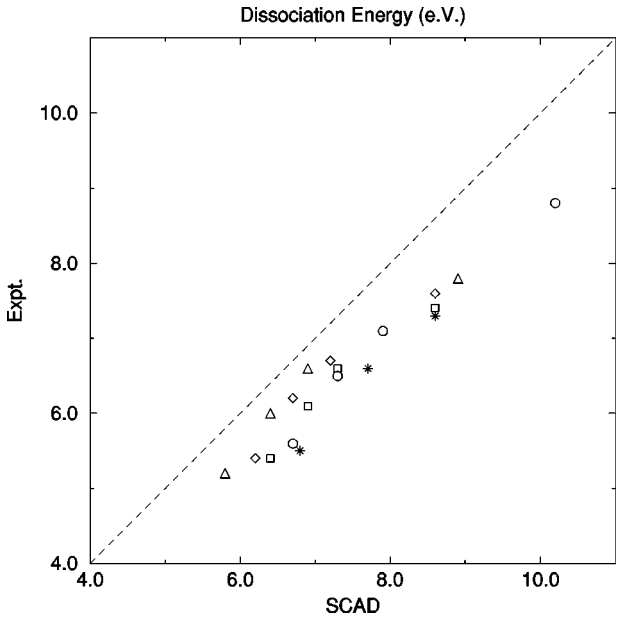

FIG. 4. Calculated vs experimental (Ref. 28) values for dissociation energy *D*, in eV, for the alkali halides: ○-Li;△-Na; ◇ -K;□-Rb; and ∗-Cs.

along with experimental values. The calculated lattice parameters are compared with experimental values in Fig. 2. The calculated values tend to underestimate *a* by a few percent. This amount of error is similar, although somewhat larger, than expected from KS band-structure methods. Shear moduli, $C_{11}-C_{12}$ and C_{44}, were determined from the quadratic dependence of total energy on volume conserving shear strains, as discussed by Mehl *et al.*[27] A nearly quadratic behavior was observed for the change in total energy for strains up to ~10%. Computed values for the elastic moduli are compared with experimental values in Fig. 3. While the agreement is reasonably good, we note that the larger discrepancies occur for the lithium and cesium compounds.

The dissociation energy *D* is the difference between the total energy calculated for the equilibrium lattice parameter and that obtained for isolated atoms. The values, listed in Table II are plotted in Fig. 4. The calculated values systematically overestimate *D* by about 10 to 15%. This is typical for KS based calculations as well.[29]

We compute the dielectric susceptibility from the polarization induced by an electric field. If the electric field is chosen to be in the *z* direction with magnitude E_z, then we

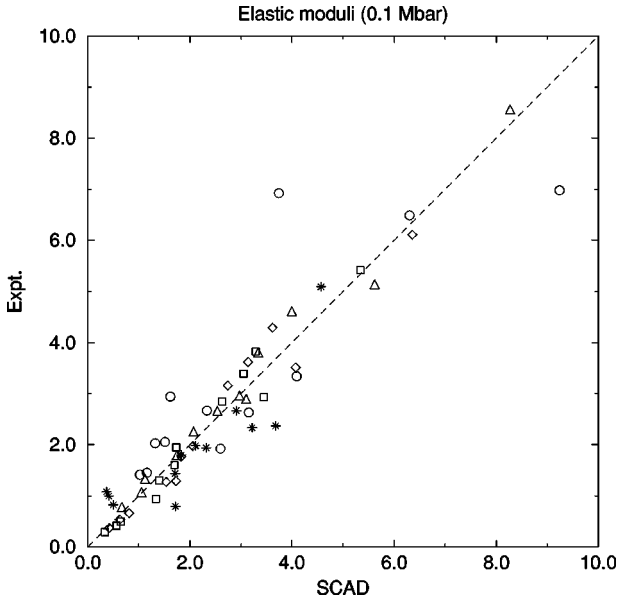

FIG. 3. Calculated vs experimental (Ref. 28) elastic moduli (bulk modulus, $C_{11}-C_{12}$ and C_{44}), in 0.1 Mbar, for the alkali halides: ○-Li;△-Na; ◇ -K;□-Rb; and ∗-Cs.

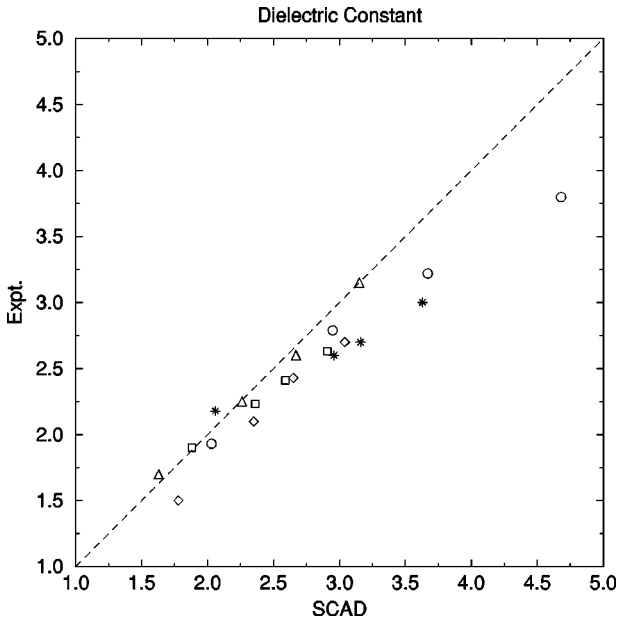

FIG. 5. Calculated vs experimental (Ref. 28) high-frequency dielectric constants for the alkali halides: ○-Li;△-Na; ◇ -K;□-Rb; and ∗-Cs.

TABLE III. Calculated and experimental (Ref. 28) Γ_- and X mode frequencies (1/cm) of alkali halides. Experimental values are expressed inside the parentheses.

	Γ_4^-	Γ_4^-	X_3^-	X_3^-	X_5^-	X_5^-
LiF	708(667)	337(315)	281(336)	505(462)	259(241)	320(347)
LiCl	440(436)	173(220)	110(170)	268(273)	132(126)	168(236)
LiBr	371(357)	137(183)	43(105)	190(220)	79(78)	141(194)
LiI	330(294)	132(141)	77(78)	146(157)	42(50)	140(144)
NaF	436(431)	237(252)	254(253)	301(293)	146(145)	255(256)
NaCl	270(269)	160(171)	148(140)	182(189)	86(84)	167(177)
NaBr	208(208)	128(133)	89(90)	143(139)	55(56)	133(134)
NaI	181(180)	120(124)	57(55)	127(142)	36(41)	122(130)
KF	351(340)	183(202)	174(162)	218(201)	96(87)	193(182)
KCl	217(217)	129(149)	107(111)	145(161)	59(62)	135(155)
KBr	167(168)	102(120)	70(71)	115(138)	39(39)	107(127)
KI	143(142)	91(107)	42(51)	101(112)	23(31)	95(108)
RbF	293(285)	147(162)	109(107)	177(182)	62(58)	156(168)
RbCl	176(174)	107(126)	73(76)	125(134)	40(42)	114(127)
RbBr	130(130)	83(93)	59(58)	92(98)	34(33)	86(95)
RbI	107(108)	71(80)	38(43)	77(82)	20(22)	74(80)
CsF	256(241)	111(133)	81(72)	126(174)	46(48)	115(145)
	Γ_4^-	Γ_4^-	X_1^+	X_3^-	X_5^+	X_5^-
CsCl	153(161)	63(103)	149(151)	52(84)	87(97)	27(43)
CsBr	110(112)	48(78)	97(97)	32(65)	82(78)	28(45)
CsI	92(85)	46(63)	71(66)	31(42)	75(74)	34(48)

TABLE IV. Calculated and experimental (Ref. 28) frequencies for high-symmetry zone-boundary modes of alkali halides (1/cm). Experimental values are expressed inside the parentheses.

	L_1^+	L_3^+	L_2^-	L_3^-	W_1	W_2	W_5	W_5
LiF	415(336)	172(200)	583(567)	233(294)	278(273)	372(357)	326(315)	379(472)
LiCl	225(210)	86(115)	378(483)	159(241)	147(152)	245(283)	175(168)	187(236)
LiBr	134(131)	47(68)	348(409)	158(200)	85(94)	228(247)	103(100)	146(210)
LiI	94(87)	34(39)	310(354)	165(168)	63(58)	217(210)	54(63)	136(147)
NaF	335(329)	196(208)	311(310)	173(172)	239(233)	208(212)	216(223)	274(292)
NaCl	180(176)	111(118)	214(228)	130(140)	132(136)	152(160)	122(120)	174(195)
NaBr	106(104)	67(69)	206(190)	125(125)	82(89)	141(173)	78(78)	139(151)
NaI	75(77)	51(51)	189(178)	122(114)	60(66)	134(145)	52(50)	125(136)
KF	292(291)	177(189)	208(208)	114(126)	209(228)	142(132)	145(145)	205(216)
KCl	158(169)	99(118)	152(149)	95(102)	117(128)	111(115)	87(88)	140(159)
KBr	98(101)	64(76)	150(157)	94(94)	76(83)	106(113)	60(57)	111(150)
KI	70(68)	46(54)	139(131)	90(97)	55(57)	100(123)	37(37)	98(106)
RbF	271(247)	165(165)	131(125)	70(73)	193(201)	89(80)	92(89)	167(179)
RbCl	148(146)	98(111)	96(99)	61(68)	113(130)	71(78)	58(57)	119(139)
RbBr	95(91)	65(75)	98(100)	63(68)	75(81)	72(77)	51(48)	89(95)
RbI	68(65)	48(54)	91(87)	61(60)	54(60)	67(69)	32(37)	76(82)
CsF	249(232)	147(145)	97(92)	47(52)	174(203)	65(53)	68(63)	123(169)
	M_2^-	M_3^-	M_5^-	M_5^-	R_5^+	R_4^-		
CsCl	29(61)	12(39)	63(90)	102(122)	101(125)	64(66)		
CsBr	16(29)	21(54)	53(61)	74(90)	70(83)	59(63)		
CsI	17(38)	25(39)	37(48)	62(76)	50(55)	54(59)		

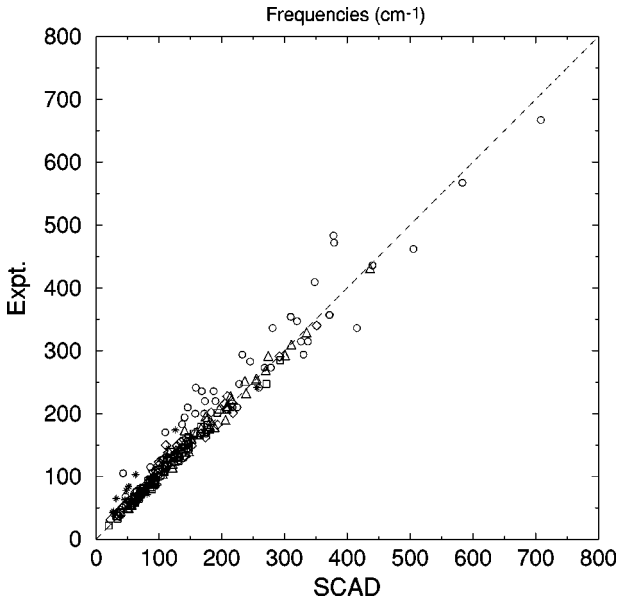

FIG. 6. Calculated vs experimental (Ref. 28) phonon frequencies as listed in Tables III and IV: ○-Li; △-Na; ◇-K; □-Rb; and *-Cs.

add the term $E_z r\sqrt{4\pi/3}$ to $v_{1,0}^{(i)}(r)$ for each ion in the unit cell. This procedure gives the same susceptibility as that obtained when the field is applied to a slab perpendicular to $\hat{\mathbf{z}}$, or if a periodic long-wavelength field in the $\hat{\mathbf{z}}$ direction is applied to supercell with the same period, as long as the change in polarization is divided by the *total* macroscopic field. For example, the change in dipole moment for ions in the interior of a slab results not only from the external field, but also from the macroscopic field due to changes in dipoles at the surfaces. In addition, phonon-dispersion curves calculated by the frozen phonon using SCAD energies have been shown to join smoothly to the longitudinal optic mode at zero wave vector.[21] We use $E_z \sim 0.001$ (Ht. atomic units) to determine the susceptibility and have verified the response is linear for fields up to this value. The computed values for dielectric constant are compared with experimental values in Fig. 5. We see the comparison is quite good with a tendency for SCAD values to be too large by $\sim 10\%$ on average.

Calculation of Born effective charge tensors $\mathbf{Z}_i^*$ using the SCAD method has been discussed by Boyer *et al.*[4] For an alkali halide there is just one value to determine because $\mathbf{Z}_i^*$ is diagonal with equal diagonal elements, and $Z^* \equiv Z_+^* = -Z_-^*$. Its value is the rigid-ion charge needed to produce the actual polarization resulting from the displacement of an ion. We use displacements of ~ 0.1 Bohr and have verified that the induced polarization has a linear dependence on displacement in this range.

We use the ''frozen phonon'' method to determine phonon frequencies. Changes in energy for distortions consistent with the phonons' symmetries[30] are calculated with the SCAD method, and these values are used to determine the quadratic coffecients and frequencies. For all but the Li compounds we used frozen modes with ~ 0.1 Bohr amplitude displacements to determind the frequencies. Values for the Li compounds were determined by least-squares fit to several energies with displacements in the range 0.1 to 0.6 Bohr. Results for the high-symmetry points in the Brillouin zone, Γ, X, L, and W for the B1 structure and Γ, X, R, and M for the B2 structure, are shown in Tables III and IV. The frequencies ω at Γ are split into longitudinal- and transverse-optical branches by the electric field associated with long-wavelength longitudinal modes. In our case the splitting is given by

$$\omega_{\mathrm{LO}}^2 = \omega_{\mathrm{TO}}^2 + \frac{4\pi e^2 (Z^*)^2}{V \epsilon_\infty \mu}, \tag{7}$$

where e is the electronic charge and μ is the reduced mass. The frequencies for all modes are compared with experimental values in Fig. 6. We see the agreement is excellent for the most part, with significantly larger discrepancies for the lithium compounds.

Many of the alkali halides transform from the B1 to the B2 structure under hydrostatic pressure. The transition pressure P_c is determined from the Gibb's energies ($G = E + PV$) for the two structures. Our calculated transition pressures are compared with experimental values and previous calculations[31] based on rigid-ion Gordon-Kim potentials in Table V. The calculation of transition pressures is very demanding for total-energy methods. Both energy differences and volume differences must be highly accurate to achieve accurate transition pressures. For example, an error in the energy difference between the two structures of one part in 10^7 of the total energy can give an error of ~ 10 kbar in P_c. We find the SCAD results give a lower energy for B1 structure for all the alkali halides. This is correct for all but the CsCl, CsBr, and CsI compounds. In the worst case, CsCl is found to have lower energy in the B1 structure by 0.0037 Ht. This is a small improvement over the spherical ion result (0.0048) obtained by Cortona.[18] He investigated the possibility that treating the heavier (Cs) ions relativistically might improve this result, but it did not. Contrary to the situation found for CsCl, our results for the Na and K compounds would indicate the B2 energies are predicted to be too low compared to the B1 energies. The source of these

TABLE V. Transition pressures in kbar for B1 to B2 structure transitions as calculated by SCAD, by preveous calculations based on rigid-ion Gordon-Kim potentials (Ref. 31) (square brackets) and from experiment (Ref. 32) (in parentheses).

	Li	Na	K	Rb	Cs
F	$>200[>200](>100)$	$>200[>200](>200)$	106[75](>100)	84[61](>100)	96
Cl	$>200[>200](>100)$	158 [46] (300)	38 [12] (20)	26 [4] (5)	$20(<0)$
Br	$>200[96](>100)$	119[30](>100)	31 [7] (19)	19 [0] (5)	$16(<0)$
I	$>200[-27](>100)$	$43[-7](>100)$	13 [−10] (19)	7 [−9] (4)	$6(<0)$

errors surely results from the use of the Thomas-Fermi approximation for overlap kinetic energy. Nevertheless, the SCAD results for P_c show a marked improvement over previous rigid-ion results.[31]

ACKNOWLEDGMENTS

Authors from the University of Nebraska received support from Nebraska-EPSCOR-NSF Grant No. EPS-9720643 and Department of the Army Grant Nos. DAAG 55-9801-0273 and DAAG 55-99-1-0106. W. N. Mei is grateful to the American Society for Engineering Education for Summer Visiting Faculty support while at NRL and to colleagues at the Center for Computational Science at NRL for their hospitality. Authors from NRL are supported by the US Office of Naval Research. We are grateful to Professor J. R. Hardy, Dr. M. Pederson, and Dr. S. Erwin for helpful discussions.

[1] L.L. Boyer and M.J. Mehl, Ferroelectrics **150**, 13 (1993).
[2] M.J. Mehl, H.T. Stokes, and L.L. Boyer, J. Phys. Chem. Solids **57**, 1405 (1996).
[3] H.T. Stokes, L.L. Boyer, and M.J. Mehl, Phys. Rev. B **54**, 7729 (1996).
[4] L.L. Boyer, H.T. Stokes, and M.J. Mehl, Ferroelectrics **194**, 173 (1997).
[5] L.L. Boyer, H.T. Stokes, and M.J. Mehl, in *First Principles Calculations for Ferroelectrics*, edited by R. E. Cohen, AIP Conf. Proc. No. 436 (AIP, New York, 1998), p. 227.
[6] L. Hedin and B.I. Lundqvist, J. Phys. C **4**, 2064 (1971).
[7] E. Clementi and C. Roetti, At. Data Nucl. Data Tables **14**, 177 (1974).
[8] A.D. McLean and R.S. McLean, At. Data Nucl. Data Tables **26**, 197 (1981).
[9] J.F. Janak, Phys. Rev. B **18**, 7165 (1978).
[10] R.G. Gordon and Y.S. Kim, J. Chem. Phys. **56**, 3122 (1972).
[11] C. Muhlhausen and R.G. Gordon, Phys. Rev. B **23**, 900 (1981).
[12] R. LaSar, Phys. Rev. Lett. **61**, 2121 (1988).
[13] G.H. Wolf and M.S.T. Bukowinski, Phys. Chem. Miner. **15**, 209 (1988); H. Zhang and M.S.T. Bukowinski, Phys. Rev. B **44**, 2495 (1991).
[14] P.J. Edwardson, Phys. Rev. Lett. **63**, 55 (1989).
[15] E. Francisco, J.M. Recio, M.A. Blanco, A. Martin Pendas, and L. Pueyo, Phys. Rev. B **51**, 2703 (1995).
[16] P. Cortona, Phys. Rev. B **44**, 8454 (1991).
[17] O.V. Ivanov and E.G. Maksimov, Phys. Rev. Lett. **69**, 108 (1992); Solid State Commun. **97**, 163 (1996); Zh. Eksp. Teor. Fiz. **108**, 1841 (1995) [JETP **81**, 1008 (1995)].
[18] P. Cortona, Phys. Rev. B **46**, 2008 (1992).
[19] D.L. Lacks and R.G. Gordon, Phys. Rev. B **48**, 2889 (1993).
[20] Listed experimental band gaps were obtained from tabulations by S.C. Erwin and C.C. Lin, J. Phys. C **21**, 4285 (1988); *Encyclopedia of Physics: Light and Matter II*, Vol. XXVI, edited by S. Flügge (Springer-Verlag, Berlin, 1958); and *CRC Handbook of Laser Science and Technology*, Vol. III, edited by M.J. Weber (CRC, Boca Raton, FL, 1986).
[21] L.L. Boyer, H.T. Stokes, and M.J. Mehl, Phys. Rev. Lett. **84**, 709 (2000).
[22] R.M. Martin, Phys. Rev. B **9**, 1998 (1974).
[23] R. Resta, Rev. Mod. Phys. **66**, 899 (1994).
[24] W. Kohn and L.J. Sham, Phys. Rev. A **140**, A1133 (1965).
[25] P. Hohenberg and W. Kohn, Phys. Rev. **136**, B864 (1964).
[26] We used a modified set of radial basis functions obtained by removing the function $re^{-\alpha r}$ with the smallest α (used in an atomic calculation to represent the $2s$ states, which are unoccupied in the SCAD calculation), to obtain reduced noise, and by adding functions of the form $e^{-\alpha r}$ to offer greater flexability to the occupied $1s$ levels.
[27] M.J. Mehl, B.M. Klein, and D.A. Papaconstantopoulos, in *Intermetallic Compounds - Principles and Practice*, Vol. 1, edited by J.H. Westbrook and R.L. Fleischer (Wiley, London, 1994), p. 195.
[28] Experimental values for lattice parameter, dielectric constant, elastic moduli, and phonon frequencies were taken from J.R. Hardy and A.M. Karo, *The Lattice Dynamics and Statics of Alkali Halide Crystals* (Plenum, New York, 1979); M. Born and K. Huang, *Dynamical Theory of Crystal Lattices* (Clarendon, Oxford, 1954); H. Bliz and W. Kress, *Phonon Dispersion Relations in Insulators* (Springer-Verlag, Berlin, 1979); and references therein. Values based on empirical models were used for cases in which experimental data for phonon frequencies were unavailable. Values for dissociation energies were taken from the tabulation of Cortona (Ref. 18).
[29] D.C. Patton, D.V. Porezag, and M.R. Pederson, Phys. Rev. B **55**, 7454 (1997).
[30] Symmetry constraints of the frozen-phonon method are imposed automatically using code based on the work by H.T. Stokes and D.M. Hatch, *Isotropy Subgroups of the 230 Crystallographic Space Groups* (World Scientific, Singapore, 1988).
[31] L.L. Boyer, Phys. Rev. B **23**, 3673 (1981).
[32] As tabulated in A.J. Cohen and R.G. Gordon, Phys. Rev. B **12**, 3228 (1975).